

The neutron radii of ^{208}Pb and neutron stars

C. J. Horowitz

Nuclear Theory Center and Dept. of Physics, Indiana University, Bloomington, IN 47405

J. Piekarewicz

Department of Physics Florida State University, Tallahassee, FL 32306

(October 29, 2018)

A new relation between the neutron skin of a heavy nucleus and the radius of a neutron star is proposed: the larger the neutron skin of the nucleus the larger the radius of the star. Relativistic models that reproduce a variety of ground-state observables can not determine uniquely the neutron skin of a heavy nucleus. Thus, a large range of neutron skins is generated by supplementing the models with nonlinear couplings between isoscalar and isovector mesons. We illustrate how the correlation between the neutron skin and the radius of the star can be used to place important constraints on the equation of state and how it may help elucidate the existence of a phase transition in the interior of the neutron star.

What determines the size of a neutron star? For spherical, static stars in hydrostatic equilibrium, the so-called Schwarzschild stars, the sole feature responsible for their size is the equation of state of neutron-rich matter. The skin of a heavy nucleus — a system 18 orders of magnitude smaller and 55 orders of magnitudes lighter than a neutron star — is also composed of neutron-rich matter, although at a lower density.

In a recent publication we studied the relation between the neutron skin of ^{208}Pb and the non-uniform solid crust of a neutron star [1]. For models with a stiff equation of state it is energetically unfavorable to separate uniform nuclear matter into regions of high and low densities. Thus models with a stiff equation of state predict low transition densities from non-uniform to uniform neutron-rich matter and consequently thinner crusts. The thickness of the neutron skin in ^{208}Pb also depends on the equation of state of neutron-rich matter. The stiffer the equation of state the thicker the neutron skin. Thus, an inverse relationship was established: the thicker the neutron skin of a heavy nucleus the lower the transition from non-uniform to uniform neutron-rich matter.

In this work we study the relation between the neutron skin of a heavy nucleus and the radius of a neutron star. Indeed, we will show that models with thicker neutron skins produce neutron stars with larger radii. Such a study is particularly timely as it complements important advances in both experimental physics and observational astronomy. Indeed, a proposal now exists at the Jefferson Laboratory to measure the neutron radius of ^{208}Pb via parity-violating electron scattering [2,3]. Moreover, a number of improved radii-measurements on isolated neutron stars, such as Geminga [4], RX J185635-3754 [5–7], Vela [8,9], and CXOU 132619.7-472910.8 [10] are now available. While these measurements are not yet accurate enough to set stringent limits on the equation of state, they represent an important first step in that di-

rection [11].

Our starting point will be the relativistic effective-field theory of Ref. [12] supplemented with new couplings between the isoscalar and the isovector mesons. The interacting Lagrangian density for this model is given by [1,12]

$$\begin{aligned} \mathcal{L}_{\text{int}} = & \bar{\psi} \left[g_s \phi - \left(g_v V_\mu + \frac{g_\rho}{2} \boldsymbol{\tau} \cdot \mathbf{b}_\mu + \frac{e}{2} (1 + \tau_3) A_\mu \right) \gamma^\mu \right] \psi \\ & - \frac{\kappa}{3!} (g_s \phi)^3 - \frac{\lambda}{4!} (g_s \phi)^4 + \frac{\zeta}{4!} g_v^4 (V_\mu V^\mu)^2 \\ & + g_\rho^2 \mathbf{b}_\mu \cdot \mathbf{b}^\mu \left[\Lambda_s g_s^2 \phi^2 + \Lambda_v g_v^2 V_\mu V^\mu \right]. \end{aligned} \quad (1)$$

The model contains an isodoublet nucleon field (ψ) interacting via the exchange of two isoscalar mesons, the scalar sigma (ϕ) and the vector omega (V^μ), one isovector meson, the rho (\mathbf{b}^μ), and the photon (A^μ). In addition to meson-nucleon interactions the Lagrangian density includes scalar and vector self-interactions. (Note that while the original model allows for ρ -meson self-interactions [12], their phenomenological impact has been documented to be small so they will not be considered in this contribution). The scalar self-interaction is responsible for reducing the compression modulus of nuclear matter from the unrealistically large value of $K = 545$ MeV [13,14], all the way down to about $K = 230$ MeV. This latter value appears to be consistent with the isoscalar giant-monopole resonance (GMR) in ^{208}Pb [15,16]. Omega-meson self-interactions have proven essential for the softening of the equation of state at high density. Indeed, without them large limiting masses for neutron stars (of about $2.8M_\odot$) are predicted, even for the softer models that provide a good description of the giant-monopole resonance [16]. This is because the GMR constrains the equation of state around saturation density but leaves the high-density behavior practically undetermined. Models that include omega-meson self-interactions soften the high-density equation of state to such a degree that limiting masses of $1.8M_\odot$ become possible [12]. Finally, the nonlinear couplings Λ_s

and Λ_v are included to modify the density-dependence of the symmetry energy [1].

We compute the neutron radius of ^{208}Pb and the radius of a “canonical” 1.4 solar-mass neutron star for all the parameter sets listed in Ref. [1]. One of these is the very successful NL3-model of Lalazissis, König, and Ring. [17]. The other models (S271 and Z271) were introduced in Ref. [1]. All the sets have been constrained to reproduce three important properties of symmetric nuclear matter at saturation: the saturation density (1.3 fm^{-3}), the binding-energy per nucleon (-16.25 MeV), and the compression modulus (271 MeV). The value of the effective nucleon mass at saturation, which is not accurately known, as well as the strength of the omega-meson self-coupling (ζ) differ in the various models [1]. This in turn permits a modification of the high-density component of the equation of state in the different models.

The energy density of symmetric nuclear matter can be computed in a mean-field approximation by solving the classical equations of motion for the meson fields. In the mean-field limit it is given by [12]

$$\begin{aligned} \mathcal{E}(\rho) = & \frac{2}{\pi^2} \int_0^{k_F} dk k^2 \sqrt{k^2 + M^{*2}} \\ & + \frac{1}{2} \left(\frac{m_s^2}{g_s^2} \right) \Phi_0^2 + \frac{\kappa}{6} \Phi_0^3 + \frac{\lambda}{24} \Phi_0^4 \\ & + \frac{1}{2} \left(\frac{m_v^2}{g_v^2} \right) W_0^2 + \frac{\zeta}{8} W_0^4. \end{aligned} \quad (2)$$

Note that the following definitions have been introduced: $\Phi_0 = g_s \phi_0$ and $W_0 = g_v V_0$. The equation of state for symmetric nuclear matter is displayed on the left panel of Fig 1. As advertised ζ , and to a lesser extent M^* , are responsible for a softening of the equation of state at high density.

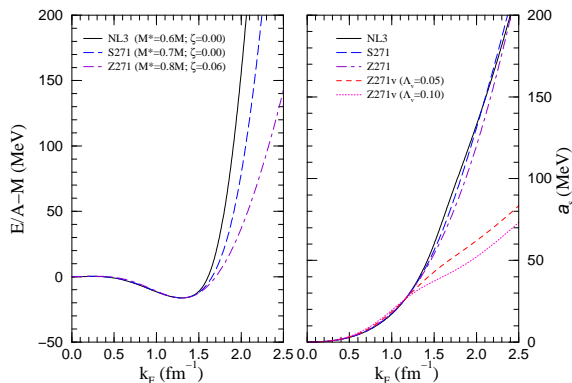


FIG. 1. Binding-energy per nucleon in symmetric nuclear matter (left panel) and symmetry energy (right panel) in the various models discussed in the text.

However, in order to compute the equation of state for neutron-rich matter one must supplement the equation

of state for symmetric nuclear matter with the symmetry energy. The symmetry energy, a positive-definite quantity, is imposed as a penalty on the system for upsetting the $N=Z$ balance. It is given by

$$a_{\text{sym}}(\rho) = \frac{k_F^2}{6E_F^*} + \frac{g_\rho^2}{12\pi^2} \frac{k_F^3}{m_\rho^{*2}}, \quad (3)$$

where $E_F^* = \sqrt{k_F^2 + M^{*2}}$ and the “effective” rho-meson mass has been defined as

$$m_\rho^{*2} = m_\rho^2 + 2g_\rho^2 \left(\Lambda_s \Phi_0^2 + \Lambda_v W_0^2 \right). \quad (4)$$

In this manner, the equation of state of neutron-rich matter may be written as

$$\frac{E}{A}(\rho, t) = \frac{\mathcal{E}(\rho)}{\rho} + t^2 a_{\text{sym}}(\rho) + \mathcal{O}(t^4), \quad (5)$$

where the neutron excess has been defined as

$$t \equiv \frac{\rho_n - \rho_p}{\rho_n + \rho_p}. \quad (6)$$

The symmetry energy is given as a sum of two contributions. The first term in Eq. (3) represents the increase in the kinetic energy of the system due to the displacement of the Fermi levels of the two species (neutrons and protons). This contribution has been fixed by the properties of symmetric nuclear matter as it only depends on the nucleon effective mass M^* . By itself, it leads to an unrealistically low value for the symmetry energy; for example, at saturation density this contribution yields $\sim 15\text{ MeV}$, rather than the most realistic value of $\sim 37\text{ MeV}$. The second contribution is due to the coupling of the rho meson to an isovector-vector current that no longer vanishes in the $N \neq Z$ system. It is by adjusting the strength of the $NN\rho$ coupling constant that one can now fit the empirical value of the symmetry energy at saturation density. However, the symmetry energy at saturation is not well constrained experimentally. Yet an average of the symmetry energy at saturation density and the surface symmetry energy is constrained by the binding energy of nuclei. Thus, the following prescription is adopted: the value of the $NN\rho$ coupling constant is adjusted so that all parameter sets have a symmetry energy of 25.7 MeV at $k_F = 1.15\text{ fm}^{-1}$ [1]. Following this prescription the symmetry energy at saturation density is predicted to be $37.3, 36.6,$ and 36.3 MeV in the NL3, S271, and Z271 models, respectively (for $\Lambda_s = \Lambda_v = 0$).

The simplicity of the symmetry energy is remarkable indeed. The contribution from the nucleon kinetic energy displays a weak model dependence through the effective nucleon mass and this dependence disappears in the high-density limit. The second term in Eq. (3) is also weakly model dependent, at least in the $\Lambda_s = \Lambda_v = 0$ limit. The reason is simple: models constrained to reproduce the

symmetry energy of nuclear matter at some average density, while maintaining the effective nucleon mass within the “acceptable” range of $0.6 \leq M^*/M \leq 0.8$, yield values for the $NN\rho$ coupling constant within 15% of each other. The weak model dependence of the symmetry energy can be observed in the right panel of Fig. 1. Note that the high-density behavior of the symmetry energy is given by

$$a_{\text{sym}}(\rho) \xrightarrow{k_F \rightarrow \infty} \frac{g_\rho^2}{12\pi^2} \frac{k_F^3}{m_\rho^2}. \quad (7)$$

As they stand now, the models lack enough leverage to significantly modify the symmetry energy. In order to remedy this deficiency one must rely on the two nonlinear couplings between the isoscalar and isovector mesons (Λ_s and Λ_v). These couplings change the density dependence of the symmetry energy by modifying the rho-meson mass as is indicated in Eq. (4). For example, for $\Lambda_v \neq 0$ the high-density behavior of the omega-meson field becomes [12]

$$W_0 \xrightarrow{k_F \rightarrow \infty} \begin{cases} \left(\frac{g_v^2}{m_v^2}\right)\rho & \text{if } \zeta = 0; \\ \left(\frac{6\rho}{\zeta}\right)^{1/3} & \text{if } \zeta \neq 0. \end{cases} \quad (8)$$

In either case ($\zeta = 0$ or $\zeta \neq 0$) the modifications are significant enough to change the qualitative behavior of the symmetry energy; the symmetry energy now grows linearly with $k_F \propto \rho^{1/3}$ rather than as k_F^3 . This change in the qualitative behavior of the symmetry energy can be seen in the right panel of Fig. 1. Note that with $\Lambda_s \neq 0$ or $\Lambda_v \neq 0$ an adjustment of the $NN\rho$ coupling constant is necessary to maintain the symmetry energy unchanged from its fixed value of 25.7 MeV at $k_F = 1.15 \text{ fm}^{-1}$. Further, the inclusion of these nonlinear terms does not affect the properties of symmetric nuclear matter as $\mathbf{b}_\mu \equiv 0$ in the $N=Z$ limit.

The procedure described above is robust in another important way. While our goal is to induce changes in the neutron radius of ^{208}Pb through a modification of the symmetry energy, we want to do so without sacrificing the success of the models in describing the binding energy and charge radius of ^{208}Pb , both of them well known experimentally (B.E. = 7.868 MeV and $R_{\text{ch}} = 5.51 \text{ fm}$) [18–20]. That this is possible may be seen in Fig. 2. In this figure the neutron and proton ground-state densities have been computed in the Z271 model for three different values of the nonlinear ω - ρ coupling Λ_v . While the softening of the symmetry energy has reduced the neutron skin of ^{208}Pb appreciably, the charge radius has changed by less than 0.005 fm.

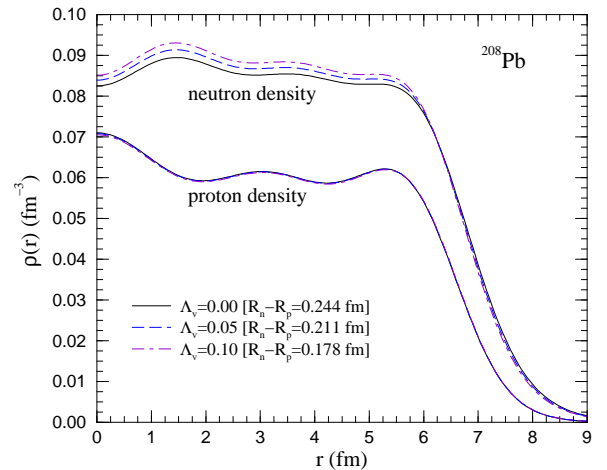


FIG. 2. Neutron and proton densities in ^{208}Pb in the Z271v model for three different values of the nonlinear ω - ρ coupling Λ_v . In all cases the root-mean-square charge radius is predicted to be $R_{\text{ch}} = 5.51 \text{ fm}$.

In Fig. 3 we show the equivalent plot but for an object 55 orders of magnitude heavier than ^{208}Pb : a 1.4 solar-mass neutron star. The density profile of such a neutron star correlates nicely with the neutron skin of ^{208}Pb . Models with a softer symmetry energy tolerate regions of large central densities thereby generating smaller radii.

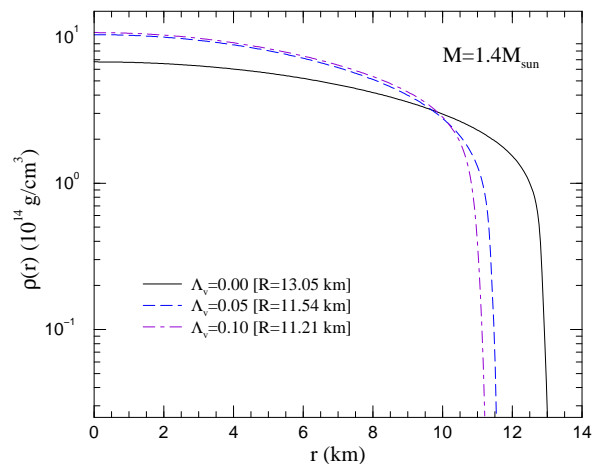


FIG. 3. Density profile for a $M = 1.4M_\odot$ neutron star in the Z271v model for three different values of the nonlinear ω - ρ coupling Λ_v .

Finally, the radius R of a 1.4 solar-mass neutron star as a function of the neutron skin $R_n - R_p$ in ^{208}Pb is displayed in Fig. 4 for the various models described in the text. All neutron-star radii were computed using the Oppenheimer-Volkoff equations for neutron-rich matter in beta equilibrium. Since this figure was generated using an equation of state for uniform matter, it may contain small errors due to an inappropriate treatment of the surface region. Note that whereas the Z271 model has been extended to include both $\Lambda_s \neq 0$ (Z271s) and

$\Lambda_v \neq 0$ (Z271v), the other two models have the σ - ρ coupling fixed at $\Lambda_s = 0$. The strong correlation between the neutron-star radius and the neutron skin in ^{208}Pb is evident: for a given parameter set R increases with $R_n - R_p$. However, as one modifies the parameter set to increase M^* or the ω -meson self-coupling ζ , the equation of state becomes softer so the pressure decreases at high density. As a result, the radius of the star becomes smaller for fixed $R_n - R_p$. For example, for a neutron skin of $R_n - R_p = 0.18$ fm, the radius of the star varies from $R \simeq 13$ km in the NL3 model all the way down to $R \simeq 11$ km in the Z271v model. Thus, we conclude that the radius of a $1.4M_\odot$ neutron star is not uniquely constrained by a measurement of the neutron-skin thickness because $R_n - R_p$ depends only on the equation of state at or below saturation density while R is mostly sensitive to the equation of state at higher densities. Yet one may be able to combine separate measurements of $R_n - R_p$ and R to obtain considerable information about the equation of state at low and high densities. For example, if $R_n - R_p$ is relatively large while R is small, this could indicate a phase transition. A large $R_n - R_p$ implies that the low-density equation of state is stiff while a small R suggests a soft high-density equation of state. The change from stiff to soft could be accompanied by a phase transition.

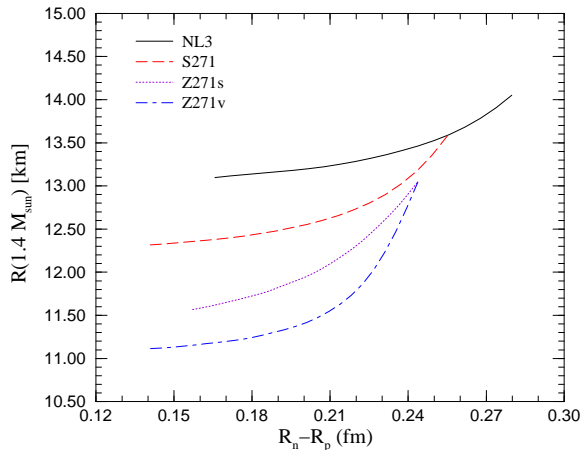


FIG. 4. Radius of a $M = 1.4M_\odot$ neutron star as a function of the neutron-minus-proton radius in ^{208}Pb for the four parameter sets described in the text.

In conclusion, relativistic effective field theories that reproduce a variety of ground-state observables have been used to correlate the radius of a 1.4 solar-mass neutron star to the neutron skin of ^{208}Pb . Nonlinear couplings between isoscalar and isovector mesons have been introduced to modify the density dependence of the symmetry energy. Models with a softer symmetry energy tolerate larger central densities and produce systems with smaller radii. Thus an important correlation is revealed: the smaller the skin-thickness of ^{208}Pb the smaller the size of the neutron star. Yet the radius of the neutron star is not uniquely constrained by a measurement of

the neutron skin in ^{208}Pb . This is because the ^{208}Pb measurement constrains the equation of state only for densities between the transition density to non-uniform matter and saturation density. In contrast, the radius of a $1.4M_\odot$ neutron star is mostly sensitive to the equation of state at high density. Yet together they provide considerable information on the equation of state. If these combined measurements reveal a large value of the neutron skin together with a small value of the star radius, this may provide strong evidence in support of a phase transition in the interior of the neutron star.

This work was supported in part by DOE grants DE-FG02-87ER40365 and DE-FG05-92ER40750.

-
- [1] C.J. Horowitz and J. Piekarewicz, Phys. Rev. Lett. **86**, (2001).
 - [2] Jefferson Laboratory Experiment E-00-003, Spokespersons R. Michaels, P. A. Souder and G. M. Urcioli.
 - [3] C. J. Horowitz, S. J. Pollock, P. A. Souder and R. Michaels, Phys. Rev. C **63**, 025501 (2001).
 - [4] A. Golden and A. Shearer, Astron. Astrophys. **342**, L5 (1999).
 - [5] Frederick M. Walter and Lynn D. Matthews, Nature **389**, 358 (1997).
 - [6] Frederick M. Walter, Astrophys. J **549**, 433 (2001).
 - [7] Jose A. Pons, Frederick M. Walter, James M. Lattimer, Madappa Prakash, Ralph Neuhäuser, and Penghui An, astro-ph/0107404.
 - [8] B. Link, R. I. Epstein and J. M. Lattimer, Phys. Rev. Lett. **83**, 3361 (1999).
 - [9] G.G. Pavlov, V.E. Zavlin, D. Sanwal, V. Burwitz, and G.P. Garmire, astro-ph/0103171.
 - [10] Robert E. Rutledge, Lars Bildstein, Edward F. Brown, George G. Pavlov, and Vyacheslav E. Zavlin, astro-ph/0105405.
 - [11] P. Haensel, Los Alamos Archive, astro-ph/0105485.
 - [12] H. Müller and B. D. Serot, Nucl. Phys. **A606**, 508 (1996).
 - [13] J.D. Walecka, Ann. of Phys. **83**, 491 (1974).
 - [14] B.D. Serot and J.D. Walecka, Adv. in Nucl. Phys. **16**, J.W. Negele and E. Vogt, eds. (Plenum, N.Y. 1986); Int. Jour. Mod. Phys. **E6**, 515 (1997).
 - [15] D.H. Youngblood, H.L. Clark, and Y.-W. Lui, Phys. Rev. Lett. **82**, 691 (1999).
 - [16] J. Piekarewicz, Phys. Rev. C **62**, 051304(R) (2000); Phys. Rev. C **64**, 024307 (2001).
 - [17] G. A. Lalazissis, J. König and P. Ring, Phys. Rev. C **55** (1997) 540.
 - [18] G. Audi and A.H. Wapstra, Nucl. Phys. **A595**, 409 (1995).
 - [19] B. Frois et al, Phys. Rev. Lett. **38**, 152 (1977).
 - [20] H. de Vries, C.W. de Jager, and C. De Vries, Atomic Data and Nucl. Data Tables, **36**, 495 (1987).